Experimental heat transfer research in enhanced flat-plate solar collectors

R. Herrero Martín[1], A. García Pinar [1], J. Pérez García*[1]

[1] Technical University of Cartagena, Cartagena, Spain
* Corresponding author. Tel: +34-968-32.59.85, Fax: +34-968-32.59.99, E-mail: pepe.perez@upct.es

Abstract: Enhancement techniques can be applied to flat-plate liquid solar collectors towards more compact and efficient designs. Tube-side enhancement passive techniques can consist of adding additional devices which are incorporated into a smooth round tube (twisted tapes, wire coils), modifying the surface of a smooth tube (corrugated and dimpled tubes) or making special tube geometries (internally finned tubes). For the typical operating flow rates in flat-plate solar collectors, the most suitable technique is inserted devices. Based on previous studies from the authors, wire coils were selected for enhancing heat transfer. This type of inserted device provides better results in laminar, transitional and low turbulence fluid flow regimes.
To test the enhanced solar collector and compare with a standard one, an experimental side-by-side solar collector test bed was designed and constructed. The testing set up was fully designed following the requirements of EN12975-2 and allow us to accomplish performance tests under the same operating conditions (mass flow rate, inlet fluid temperature and weather conditions). In this work the preliminary results obtained are presented and the standardized efficiency curve is shown for both tested solar collectors. A relevant improvement of the efficiency has been reported and quantified through the useful power ratio between enhanced and standard solar collectors.

Keywords: *heat transfer enhancement, wire-coil inserts, liquid flat plate solar collector*

Nomenclature

A_A	*Absorber area*	m^2
α_{A1}	*Thermal losses coefficient*	W/m^2K
c_p	*Specific heat of working fluid*	J/kgK
Q_{useful}	*Useful power*	W
Q	*Flow rate*	m^3/s
G	*Global irradiance*	W/m^2
η	*Thermal efficiency*	
η_A	*Thermal efficiency based on absorber area*	
η_O	*Optical efficiency coefficient*	
η_{OA}	*Optical efficiency coefficient*	
ρ	*Fluid density*	kg/m^3
t_a	*Ambient temperature*	ºC
t_{in}	*Inlet temperature*	ºC
t_{out}	*Outlet temperature*	ºC
t_m	*Mean temperature* $t_m = t_{in} + \Delta t/2$	ºC
T^*_m	*Nondimensional temp.* $T^*_m = (t_m - t_a)/G$	
τ	*Transparent cover transmittance*	
α	*Absorptance of absorber plate*	
F_R	*Heat removal factor*	

1. Introduction

In industrial applications, a set of enhancement techniques are widely used to improve the performance of heat exchangers. Enhanced surfaces can be used to increase heat exchange, reduce the size of equipments or save pumping power. Thermal liquid solar collectors are potential candidates for enhanced heat transfer, but not many studies have focused on this aspect. The vast majority of works carried out applying enhancement techniques to improve solar collector performance deal with air collectors, mainly inserting artificial roughness within the exchange surfaces [1, 2, 3].

Regarding liquid solar collectors just a few studies have focused on enhancement techniques. Kumar and Prasad [4] presented a remarkable work inserting twisted tapes in a serpentine solar collector. They investigated the effect of the twisted-tape geometry, different mass flow rates and intensity of solar radiation on thermal performance. The authors observed that heat losses were reduced (due to the lower value of the plate temperature) and consequently an increase on the thermal efficiency was observed.

Recently, Jaisankar et al [5] performed an experimental investigation of heat transfer, friction factor and thermal performance on a tube-on-sheet solar panel with twisted-tape insert devices. They also investigated the effect of the twisted-tape geometry for different Reynolds and intensity of solar radiation. The concluded that when twist ratio is increased, the swirl generation is decreased and both heat transfer and friction factor are minimized. Jaisankar et al also carried out several experimental investigations of heat transfer, friction factor and thermal performance of thermosyphon solar water heater systems fitted with twisted- tape insert devices. [6, 7, 8] The authors found that the heat transfer enhancement in the twisted tape collector was higher than in the standard collector.

Also Hobbi and Siddiqui [9] conducted an indoor experimental study to investigate the impact of several insert devices on the thermal performance of a f lat-plate solar collector. They studied different passive heat enhancement devices: twisted strips, coil-spring wires and conical ridges. They observed no appreciable difference in the heat transfer to the collector fluid and concluded that the applied passive methods based on t he enhancement of shear-produced turbulence were ineffective in augmenting heat transfer to the collector fluid.

In spite of the fact that many of the previous works within liquid collectors employed twisted tapes as inserted devices, basically due to the existence of well known design correlations [10, 11, 12], the use of other passive tube-side techniques such as wire coils still unexplored. Regarding the aforementioned fact, Webb and Kim [13] also pointed out that the existence of design correlations does not mean, however, that the twisted tape insert is the best insert device. As Garcia mentions [14, 15], wire coils are especially suitable for enhancing heat transfer in laminar, transition and low turbulent flow regimes. In a previous work from the authors, a numerical simulation methodology to study the heat transfer enhancement in a tube-on-sheet solar panel with wire-coil inserts, using TRNSYS as the simulating tool was developed. A parametric study was also performed to relate the fluid and flow characteristics with the heat transfer enhancement by wire-coil inserts. It was shown that the enhanced collector increased useful power in the whole range of mass flow rate when using water as the working fluid [16].

The purpose of the present work is then to characterize a flat-plate solar panel with wire-coil insert devices in terms of heat transfer, friction losses and thermal performance and compare this enhanced collector with a s tandard collector under the same operating and weather conditions. To test the enhanced solar collector and compare with a standard one, an experimental side-by-side solar collector test bed was designed and constructed. The testing set up w as fully designed following the requirements of EN 12975-2 [17]. A relevant improvement of the standardized efficiency curve has been reported. Furthermore, the ratio of useful power and pressure drop between the enhanced and the standard solar collector for different flow rates and operating conditions were computed.

2. Experimental set-up

The experimental setup was designed to carry out simultaneously the thermo-hydraulic characterization of two solar collectors (an enhanced collector with wire-coil inserts and a standard collector) under the same operating (mass flow rate, inlet fluid temperature) and weather conditions. It is located in Cartagena, southeastern Spain (Latitude N'3736, Longitude W'00059). Furthermore, this facility was built in agreement with the requirements of standard EN 12975-2 [17]. A schematic layout of the test bed constructed is shown in Figure 1.

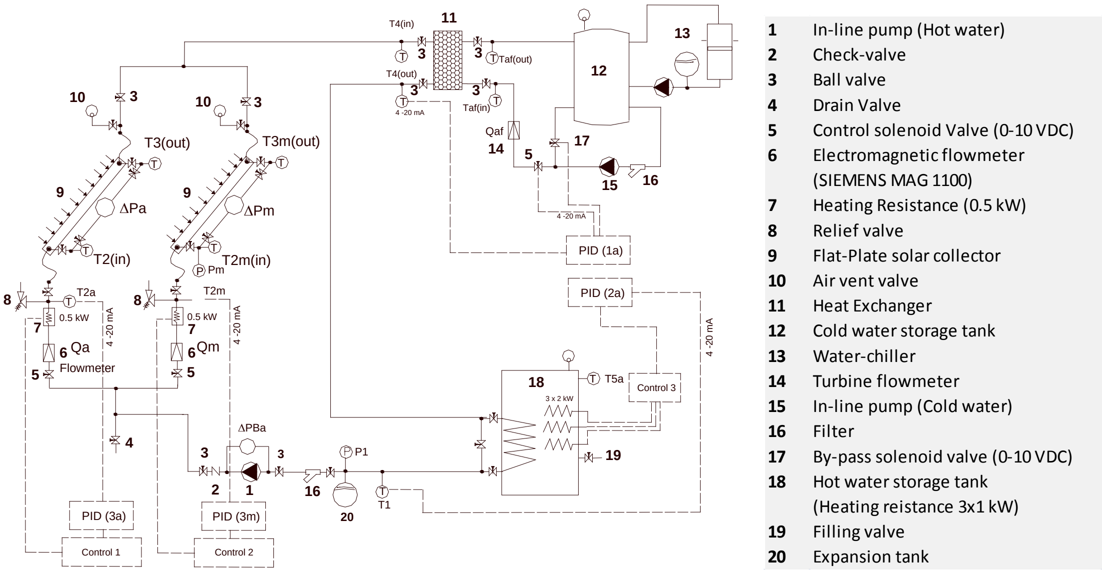

Fig. 1. Experimental set-up

The main components of the experimental setup are the two sheet-and-tube flat-plate solar water heaters with 9 parallel tubes (risers) on the back of the absorber plate, as it is detailed in Fig. 2. T he risers are connected at the top and bottom by headers to homogenize flow distribution and static pressure at inlet and outlet sections. Both collectors have a single glass cover; their technical specifications are summarized in Table 1.

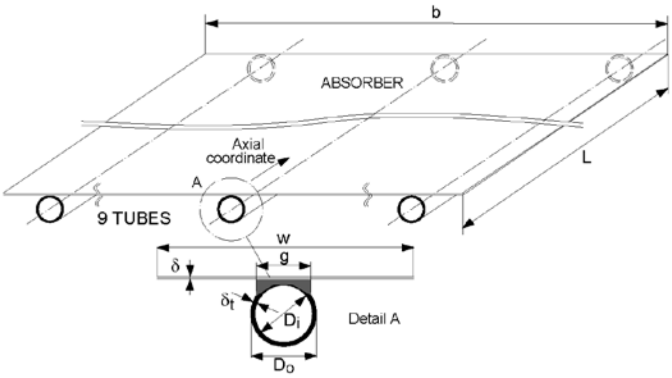

Fig. 2. Sheet-and-tube tested solar collector configuration

Table 1. Main characteristics of the flat-plate solar collectors

	Material properties		**Geometrical data**		
k_{abs}	209.3 W/mK (Aluminum)	D_i	0.007 m	N_G	1
k_{tube}	372.1 W/mK (Copper)	w	0.1227 m	N_{tubes}	9
ε_g	0.88 (Glass)	g	0.0035 m	A_C	2.022 m^2
τ_g	0.93 (Glass)	δ_{abs}	0.0005 m	A_{edge}	0.2348 m^2
k_{ins}	0.05 W/mK	δ_{tube}	0.0005 m	L_t	1.83 m
ε_{abs}	0.05 (Miro-Therm)	δ_{ins}	0.025 m	β	45º
		α_{abs}	0.95 (Miro-Therm)		

One of the solar collectors was modified inserting wire–coils within their risers. A wire coil of dimensionless pitch p/D=1 and wire-diameter e/D=0.0717 was chosen (Fig. 3). This geometry showed good overall thermohydraulic behaviour for the operating conditions in solar collectors according to Garcia [15] work.

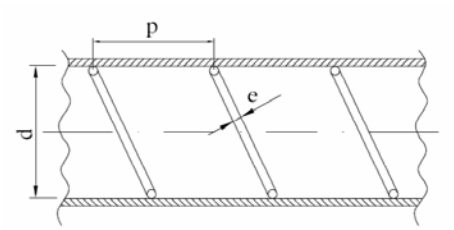

Fig. 3. Sketch of the helical-wire-coil fitted in the raisers of the modified solar collector.

2.1 Instrumentation

The instrumentation was selected and mounted according to the standard EN 12975–2 requirements. Thermorresistance Pt100 class 1/10 DIN A were used to measure the inlet and outlet fluid flow temperatures. To measure the flow rate and the pressure drop through the collectors, electromagnetic flowmeters (Siemens MAG1100 DN 3) and differential pressure transmitters (SMAR) with different configurable ranges were used. Regarding the weather conditions: 3 PSP class I thermoelectric pyranometers were employed to measure the solar irradiance (global irradiance in the aperture plane, global irradiance on the horizontal plane and the other one has a shading band to measure diffuse horizontal solar irradiance). Velocity and wind direction were measured with an ultrasonic anemometer (Windsonic from Gill Instruments Ltd). Ambient temperature, humidity and pressure were also measured. In Table 2 the main characteristics of the selected instrumentation are summarized.

2.2 Uncertainty propagation

We follow the criteria of ISO GUM (Guide to the expression of Uncertainty in Measurement) [18] to derive the equation for thermal efficiency proposed in EN 12975-2 and uncertainty propagation assessment. When the tests are accomplished in steady state, the thermal efficiency can be expressed as Eq. (1).

$$\eta_A = \frac{\dot{Q}_{\text{useful}}}{GA_A} = \frac{Q\rho_{(t)}c_{p(t)}\left(t_{out} - t_{in}\right)}{GA_A} \tag{1}$$

The standard uncertainty of each magnitude is shown in Table 2. The uncertainty of each magnitude is a combination of the uncertainties of Type A evaluation, associated to the standard deviation of the mean of the repeated observations, and of Type B, evaluated from scientific statement based on the calibration available information. According to the uncertainty propagation study carried out, it can be concluded that the initial uncertainties are slightly amplified and the expanded uncertainty at a 95% confidence level are ±0.1% for non-dimensional temperature T^*_m and ±0.9% for thermal efficiency η .

3. Thermal performance calculations according to standard EN 12975-2

The useful power is calculated according to Eq. (2).

$$\dot{Q}_{useful} = Q\rho_{(t)}c_{p(t)}\left(t_{out} - t_{in}\right) \tag{2}$$

where, the fluid density and the specific heat are evaluated at the mean fluid temperature $t_m = t_{in} + \Delta t/2$, and the thermal efficiency can also be expressed according to Eq. (3) as a function of global irradiance intercepted, absorber area and useful power.

$$\eta = \frac{\dot{Q}_{useful}}{GA_A} \tag{3}$$

Table 2 . Instrumentation description and uncertainty.

Magnitude	Sensors	Instrumentation	Uncertainty
Solar Irradiation	3	1st Class Kipp&Zonnen CMP6 Pyranometer Shadow band (Diffuse Irradiation)	±0.,1%
Ambient Temperature	1	Pt100 3w	±0.1ºC
Ambient Pressure	1	Piezorresistive barometer	± 0,4 mbar a 20ºC
Humidity	1	Capacitive sensor	±2%
Wind velocity and direction	1	WindSonic Gill Instrument (Vel. interval 0-60 m/s) (Vel. Direction 0-359º)	± 2% Velocity ± 3% Direction
Inlet and Outlet Fluid Temperature	4	Pt100 4w Class 1/10 DIN A	± 0,03 ºC
Flow Rate	2	Electromagnetic Flowmeter Siemens MAG 1100 Transmitter MAG 6000	± 0,25 %
Differential Pressure	2	Differential pressure transmitter SMAR D0 type (-4 to +4 inch H_20) Standard collector D1 type (0-20 inch H_20) Enhanced collector	± 0,1 % of Span
Absolute pressure	1	Piezorresistive transducer	± 0,5 %

The thermal efficiency η can be correlated with the reduced temperature, $T^*_m=(t_m-t_a)/G$ using linear $\eta = \eta_0 - a_1 T^*_m$ or quadratic regressions $\eta = \eta_0 - a_1 T^*_m - a_2 G T^{*2}_m$, based on absorber or aperture area. The experimental data obtained show a good linear correlation (R^2=0.9874 for the standard solar collector, and R^2=0.9282 for the enhanced solar collector). These linear correlations are simpler and more useful in engineering applications. Additionally, their coefficients are independent of global irradiance.

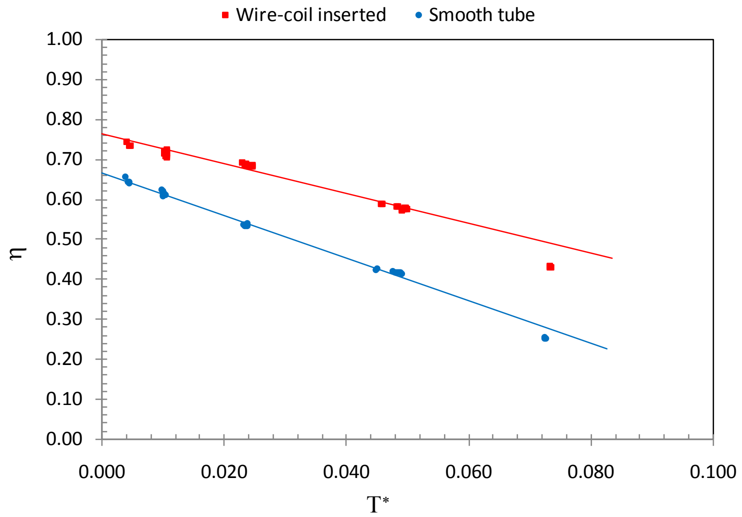

Fig. 4. Thermal efficiency curves for standard and enhanced flat-plate solar collectors (0.04 kg/s)

In Fig. 4 the standardized thermal efficiency curves for both standard and enhanced flat-plate solar collectors are shown. It can be observed that a significant improvement in the thermal efficiency of the solar collector with wire-coil inserts is achieved. Note that in the enhanced solar collector the optical efficiency coefficient η_{OA} is about 15% higher and the thermal losses coefficient α_{A1} is lower than in the standard one (Table 4). This effect can be due to the enhancement of heat transfer between the absorber plate and the working fluid which reduces its temperature and as a consequence, the thermal losses decrease. The uncertainty of the regression coefficients have also been assessed according to the methodology proposed by Coleman and Steele [19].

Table 4. Linear correlation coefficients and their uncertainties (95% I.C)

	Standard collector		Enhanced collector	
	Coefficient	Uncertainty	Coefficient	Uncertainty
η_{0A}	0.6670	0.44 %	0.7654	3.97 %
a_{1A}	-5.3410	1.71 %	-3.7640	0.52 %

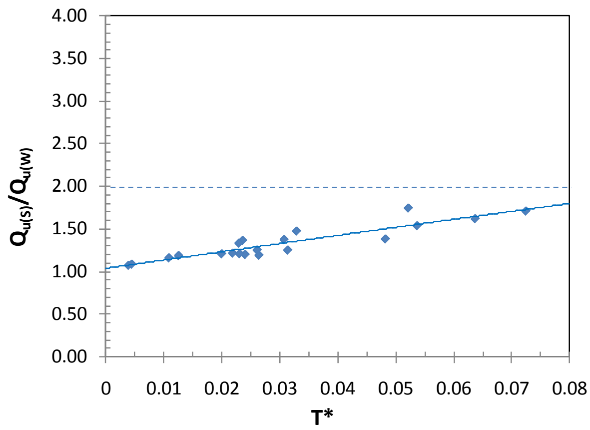

a)

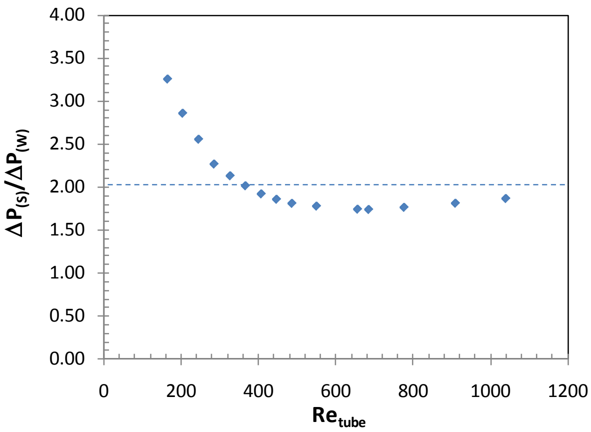

b)

Fig. 5. Ratios between standard and enhanced solar collectors a) Useful power versus non-dimensional temperature, and b) Loss pressure versus Reynolds number inside raisers

In Fig. 5 a) the useful power ratio between the enhanced and the standard solar collector is showed for different flow rates (0.016÷0.04 kg/s) and operating conditions ($520 \leq Re_{tube} \leq 2340$). It can be observed that there is a linear dependence between the useful power ratio and the non-dimensional temperature. For increasing values of T^* the ratio of useful power is higher. This is due to the fact that the wire-coil insert lowers the absorber temperature reducing the thermal losses. This confirms the results from the previous numerical simulations carried out by the authors. [16] In Fig. 5 b) the pressure loss ratio between both collectors is represented. For Reynolds numbers higher than 500, inside the raisers, the pressure loss ratio remains constant at about 1.8. This increase in pumping power is compensated with an improvement in thermal efficiency, which would be especially suitable for large installations in which several solar collectors are connected in parallel. In this type of configuration an accumulative increase in thermal power is obtained, while the pressure loss remains the same in all the solar collectors, and thus, this configuration would enable optimum operation and would be the best-practice approach.

Nevertheless, in order to establish the optimum operating range within enhanced solar collectors with wire-coil inserts, a heat exchangers performance evaluation criterion has to be employed. A modified criterion (R3m) was proposed by the authors [16]. This criterion stands for the increasing useful power obtained in the enhanced and the standard collector at equivalent operating regimes to satisfy the constraint of equal pumping power. To compute this parameter further efficiency and friction factor tests are being carried out.

4. Conclusions

An experimental side-by-side solar collector test bed was designed and constructed to characterize the thermo-hydraulic behaviour of a standard and an enhanced solar collector under the same testing conditions (operating parameters and radiant conditions). The facility was built in agreement with the requirements of standard EN 12975 to carry out thermal performance and pressure drop tests.

The thermal efficiency curves of two solar collectors, a standard and an enhanced collector were obtained. The enhanced collector was modified inserting spiral wire coils of dimensionless pitch p/D=1 and wire-diameter e/D=0.0717 within each riser. The thermal efficiency increments depend on the operating flow rates. For a flow rate of 144 l/h (0.04 kg/s) the efficiency optical factor was found to increase by 15%. The collector with wire-coil inserts enhances heat transfer and as a consequence the absorber temperature is reduced. This means a reduction in the thermal losses as well as a decrease of the loss coefficient by 30%. However, an increase in terms of friction losses is observed and thus pumping power rises.
In order to account for the overall enhancement (thermo-hydraulic performance) that wire-coil inserts promote in the solar collector, the ratio of useful power and pressure loss between both solar collectors were computed. For increasing values of T* the ratio of useful power is higher and reaches values up to 1.8. For Reynolds numbers higher than 500, inside the raisers, the pressure loss ratio remains constant at about 1.8. The increase in pumping power is compensated with an improvement in thermal efficiency, which would be especially suitable for collectors connected in parallel. This configuration would enable optimum operation and would be the best-practice approach.

As a final conclusion, according to the present work, wire-coil devices can be successfully inserted within the flow tubes in solar water heaters for enhancing heat transfer rate.

Acknowledgements
This research is supported by the Spanish Regional Agency “ARGEM” (Agencia de Gestión de la Energía de la Región de Murcia) and by the “Fundación Séneca” in the frame of the research project “Design and development of an enhanced flat plate solar collector. Thermal efficiency evaluation and thermohydraulic characterization” Reference number: 08731/PI/08.

References

[1] A. Kumar, J.L. Bhagoria, R.M. Sarviya, Heat transfer and friction correlations for artificially roughened solar air heater duct with discrete W-shaped ribs. Energy Conversion and Management, 50 (8), 2009, pp. 2106-2117.

[2] S. B. Bopche, M. S. Tandale. Experimental investigations on heat transfer and frictional characteristics of a turbulator roughened solar air heater duct. International Journal of Heat and Mass Transfer, 52 (11-12), 2009, pp. 2834-2848.

[3] K.R. Aharwal, B. K. Gandhi, J.S. Saini. Heat transfer and friction characteristics of solar air heater ducts having integral inclined discrete ribs on absorber plate. International Journal of Heat and Mass Transfer, 52, (25-26), 2009, pp. 5970-5977.

[4] A. Kumar, B. N. Prasad. Investigation of twisted tape inserted solar water heaters—heat transfer, friction factor and thermal performance results. Renewable Energy, 19 (3), 2000, pp. 379-398.

[5] S. Jaisankar, T.K. Radhakrishnan, K.N. Sheeba. Experimental studies on heat transfer and friction factor characteristics of forced circulation solar water heater system fitted with helical twisted tapes. Solar Energy, 83 (11), 2009 , pp. 1943-1952.

[6] S. Jaisankar, T.K. Radhakrishnan, K.N. Sheeba. Studies on heat transfer and friction factor characteristics of thermosyphon solar water heating system with helical twisted tapes. Energy 34, 2009, pp. 1054–1064.

[7] S. Jaisankar, TK. Radhkrishnan, KN. Sheeba. Experimental studies on heat transfer and friction factor characteristics of thermosyphon solar water heater system fitted with spacer at the trailing edge of twisted tapes. Applied Thermal Engineering, 29(5–6), 2009, pp. 1224–31.

[8] S. Jaisankar, T.K. Radhakrishnan, K.N. Sheeba, S. Suresh. Experimental investigation of heat transfer and friction factor characteristics of thermosyphon solar water heater system fitted with spacer at the trailing edge of Left–Right twisted tapes. Energy Conversion and Management, 50 (10), 2009, pp. 2638-2649.

[9] A. Hobbi, K. Siddiqui. Experimental study on the effect of heat transfer enhancement devices in flat-plate solar collectors. Int. J. of Heat and Mass Transfer 52, 2009, pp. 4650–4658.

[10] P.S. Bandyopadhyay, U.N. Gaitonde, S.P. Sukhatme. Influence of free convection on heat transfer during laminar flow in tubes with twisted tapes. Exp. Therm. Fluid Sci. 45, 1991, pp. 577–586.

[11] R.M. Manglik, A.E. Bergles. Heat transfer and pressure drop correlations for twisted-tape inserts in isothermal tubes: Part II –transition and turbulent, J. Heat Transfer, 115, 1993, pp.890–896.

[12] R.M. Manglik, S. Maramraju, A.E. Bergles. The scaling and correlation of low Reynolds number swirl flows and friction factors in circular tubes with twisted tape inserts, J. Enhanced Heat Transfer, 8, 2001, pp. 383–395.

[13] R. L. Webb , N-H. Kim. Principles of Enhanced Heat Transfer, 2nd ed., Taylor & Francis, New York, 2005.

[14] A. García, P.G. Vicente, A. Viedma. Experimental study of heat transfer enhancement with wire coil inserts in laminar-transition-turbulent regimes at different Prandtl numbers. International Journal of Heat and Mass Transfer, 48 (21-22), 2005, pp. 4640-4651.

[15] A. García, J. P. Solano, P. G. Vicente, A. Viedma. Enhancement of laminar and transitional flow heat transfer in tubes by means of wire coil inserts. International Journal of Heat and Mass Transfer, 50, (15-16), 2007, pp. 3176-3189.

[16] R. Herrero Martín, J. Pérez-García, A. García, F. J. García-Soto, E. López-Galiana Simulation of an Enhanced Flat-Plate Solar Liquid Collector with wire-coil insert devices. Manuscript accepted for publication in Solar Energy.

[17] EN 12975-2:2006 "Thermal Solar Systems and Components –Solar Collectors – Part 2 test methods".

[18] ISO/IEC Guide 98, Guide to the Expression of Uncertainty in Measurement (GUM), International Organization for Stand. (ISO), Geneva, Switzerland, 1995, pp. 9–78.

[19] Coleman, H.W, Steele, W. Experimentation and Uncertainty Analysis for Engineers, John Wiley & Sons. 1999, 2nd Ed., New York. ISBN 0-471-12146-0, pp 202-235